DEEP-LEARNING-BASED SNOWPACK MAPPING AND FORECASTING WITH GROUND OBSERVATIONS: A CASE STUDY USING A WIRELESS-SENSOR NETWORK IN THE AMERICAN RIVER BASIN

Guotao Cui[1] and Roger Bales[1]

EXTENDED ABSTRACT

Mountain snowpack in the Sierra Nevada is a major source of California's water supply. Basin-scale snowpack is crucial hydrologic information for water-resources decision making (Bales et al., 2006), e.g. reservoir operation and flood control. In particular, during precipitation events associated with atmospheric rivers, rain-on-snow-melted snow can significantly augment basin runoff (Henn et al., 2020), highlighting the importance of near-real-time estimates and forecasts of snowpack for decision-making support. This study presents an approach based on a deep-learning Long Short-Term Memory (LSTM) model and a bias-correction method using ground snow measurements for snow mapping and forecasting. The approach is evaluated in the upper American River basin (elevation ≥1500 m, Figure 1).

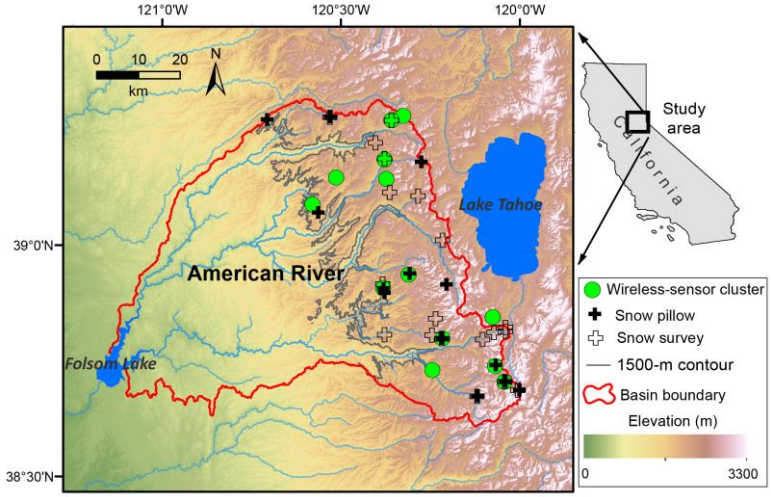

Figure 1. Location of the American River basin and snow observatories, including wireless-sensor clusters, snow pillows, and snow surveys.

SNOW OBSERVATIONS

Point-scale Snow Water Equivalent (SWE) is measured by automatic daily snow pillows and manual monthly snow surveys from an operational network, with real-time data hosting in California Data Exchange Center (CDEC, http://cdec.water.ca.gov). We collected snow data from 14 snow pillows and 19 survey sites across the American River basin (Figure 1). Meanwhile, a research network consisting of 13 wireless-sensor clusters provides snow-depth measurements and other hydrologic attributes across the upper basin (Zhang et al., 2017). Each wireless-sensor cluster consists of 10 sensor nodes distributed within 1 km^2, showing snow-depth heterogeneity due to varying physiographic conditions (Figures 2a-b). As complementary to SWE from snow pillows and surveys (Figures 2c-d), the wireless-sensor network offers extensive snow-depth data encompassing fine-scale variabilities (Cui et al., 2020). Since this study primarily focuses on basin-scale SWE mapping at a 1-km resolution, we averaged snow-depth data within each cluster and estimated SWE amount using snow density,

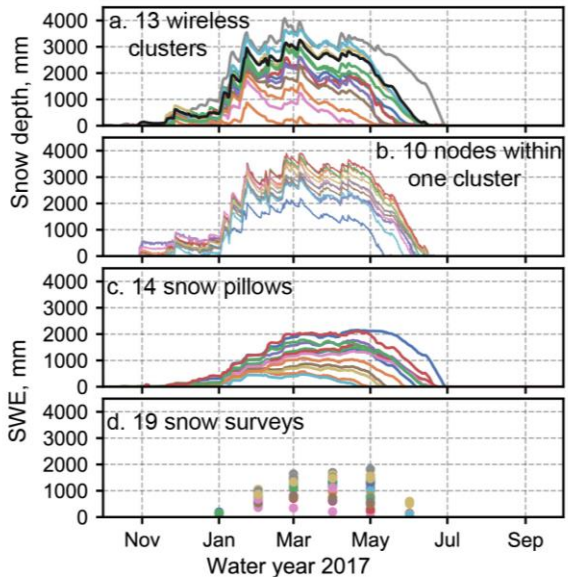

Figure 2. Snow measurements from both research (a-b) and operational (c-d) networks: (a) 13 wireless-sensor clusters network, (b) 10 sensor nodes within one cluster, (c) snow pillows, and (d) snow surveys.

Paper presented Western Snow Conference 2021
[1] Guotao Cui, Sierra Nevada Research Institute, University of California, Merced, CA, gcui3@ucmerced.edu
[1] Roger Bales, Sierra Nevada Research Institute, University of California, Merced, CA, rbales@ucmerced.edu

which was calculated using co-located snow-depth and SWE measurements. These SWE data from both the operational and research networks provide fundamental point-scale information on headwater snowpack.

SNOW MAPPING APPROACH

To estimate and forecast snowpack, we propose a snow mapping approach based on a deep-learning LSTM model and data assimilation using bias correction (Figure 3). In general, the approach consists of three main parts.

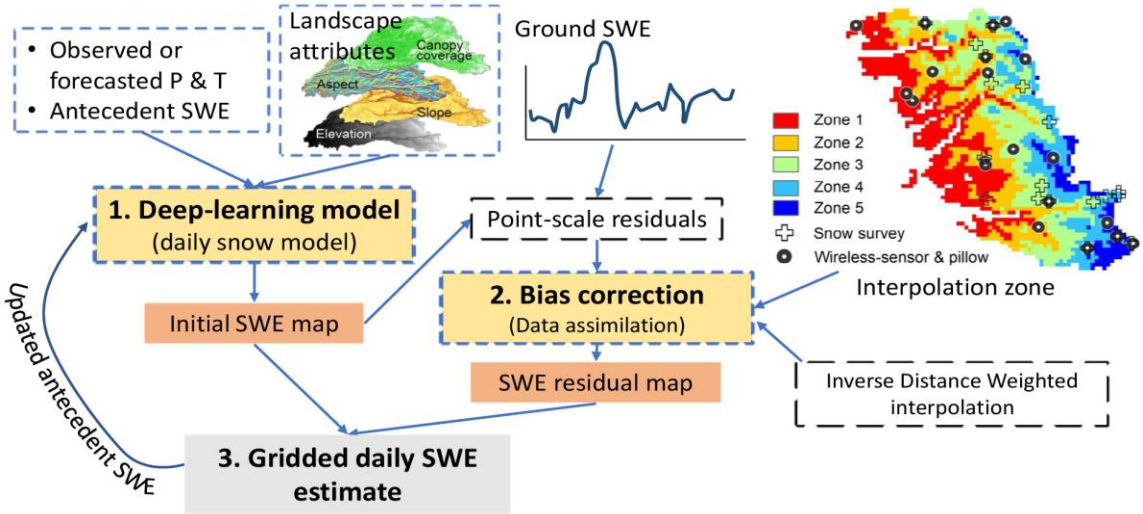

Figure 3. Snow mapping approach based on a deep-learning Long Short-Term Memory (LSTM) model and a bias-correction method using ground snow measurements.

First, an LSTM model was trained to predict initial SWE maps at day t, using precipitation and temperature at day t, antecedent SWE at one day prior (i.e. at day $t-1$), and landscape attributes. As a type of recurrent neural network for time-series prediction, the deep learning LSTM model has been successfully used to simulate natural systems, e.g. runoff at ungauged basins (Kratzert et al., 2019). Daily gridded SWE estimates from snow reanalysis data (Margulis et al., 2016) were used as model target data. Dynamic input data included daily precipitation and temperature, either from observation-based PRISM dataset (http://www.prism.oregostate.edu) or weather forecasts. Landscape attributes that affect snow accumulation and ablation were used as static inputs, e.g. elevation, aspect, slope, and canopy cover (Zheng et al., 2018). All data were resampled with a resolution of 1 km. The LSTM model can be considered a surrogate snow model trained by snow reanalysis data, providing initial SWE estimates.

Second, a bias-correction method using SWE observations was applied to the initial SWE map from the LSTM model. Point-scale SWE residuals were calculated as the difference between the initial SWE map and ground SWE observations from the wireless-sensor network and snow pillows. To account for spatial variability of mountain snow, the upper American River basin was divided into 5 different snow zones, determined by a Gaussian Mixture Model (GMM, Oroza et al., 2016) using elevation and the ratio of April 1st SWE to annual precipitation. Hence, the SWE residual map can be obtained by interpolating point-scale SWE residuals at each snow zone using Inverse Distance Weighting (IDW). The daily bias-corrected SWE map summarized the initial SWE map and SWE residual map, such that the LSTM SWE estimates were nudged to ground snow observations.

Third, the daily bias-corrected SWE map was then used as the antecedent SWE state for estimating SWE at next time step by the LSTM model. The snow mapping approach can also run with current SWE (at day t) and forecasted precipitation and temperature data (at day t+1) to predict SWE estimates (at day t+1). For example, the California Nevada River Forecast Center (CNRFC, https://www.cnrfc.noaa.gov/) provides weather forecast data at a resolution of ~4 km. We can evaluate the performance of the approach using forecast data with a 1-day leading time.

EVALUATION OF SNOW ESTIMATES

The LSTM model showed good predictability for the testing period (water year 2012-2016), after training and validating the model with snow reanalysis data in 1985-2006 and in 2007-2011, respectively. Figure 4a

demonstrates that predicted SWE from the LSTM model without bias correction are in good agreement with target snow reanalysis data, with a coefficient of determination R^2 of 0.99 and Root Mean Square Error (RMSE) of 5.9 mm. The SWE differences between the LSTM model and reanalysis tend to be more noticeable at some pixels with less snow (Figure 4b), indicating potential higher uncertainty of SWE prediction in lower elevations where rain-snow transition often occurs. Note that the antecedent SWE inputs for the LSTM model were forced by the snow reanalysis data for model training, validation, and testing (Figures 4a-b). For continuous snow mapping applications, the LSTM model recurrently uses predicted SWE as antecedent SWE inputs. As illustrated by Figures 4c-d, the LSTM model tends to underestimate the basin SWE compared to ground snow observations, showing that model biases accumulate since predicted SWE was recurrently used as antecedent SWE state in LSTM. This also highlights the need for bias correction.

By applying the bias correction, the Nash-Sutcliffe Efficiency (NSE) of basin-averaged SWE was improved from 0.61 to 0.96 (Figure 4c). Thus, the proposed snow mapping approach (i.e. LSTM plus bias-correction) provides significantly better SWE estimates than the LSTM-only model, compared to snow observations from the wireless-sensor network and snow pillows. In addition, we independently evaluated SWE estimates using SWE measurements from monthly snow surveys, which were excluded in the bias-correction procedure. SWE estimates from both reanalysis and LSTM model were noticeably lower than snow survey data (Figure 4d). The LSTM plus bias correction can provide SWE estimates matching snow surveys, and show comparable performance as the SNOw Data Assimilation System (SNODAS).

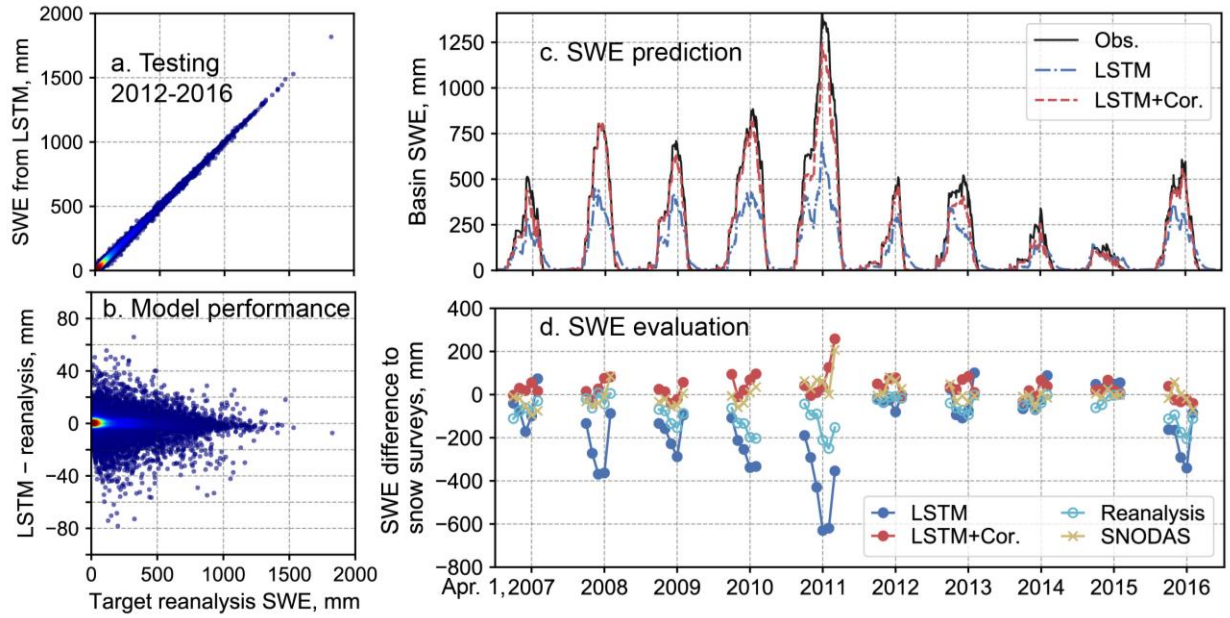

Figure 4. Performance of deep-learning LSTM model (a-b) and evaluation of time-series SWE prediction (c-d). Pixel-level (1-km) SWE estimates using the LSTM model for testing (2012-2016) are plotted in panel a, and differences to target reanalysis are shown in panel b. Point density is illustrated by colors with red indicating more points. Panel c shows basin-averaged SWE estimates from the proposed snow mapping approach (labeled as LSTM+Cor.) in comparison to the LSTM-only approach and ground observations. Panel d plots the mean difference of SWE estimates compared to monthly SWE at 19 snow survey sites.

SWE PREDICTION USING WEATHER FORECAST DATA

Basin-averaged SWE estimates from models using precipitation and temperature from observation-based PRISM and weather forecasts with 1-day leading time were comparable (Figures 5a and 5d), since bias correction nudges SWE estimates towards ground observations. However, SWE estimates from modeling with forecast data showed a slightly larger mean difference (44 mm, Figure 5b) to snow surveys than did those with PRISM data (22 mm). SWE maps exhibit similar spatial patterns of the interpretation snow zones (Figures 5c and 3).

In summary, the data-driven deep-learning model can provide snow maps, and bias correction using ground snow measurements significantly improves estimates. With daily bias correction, basin-scale SWE estimates are not sensitive to forcing data from either observation-based dataset or weather forecasts. The proposed snow mapping approach can be extended for real-time applications, providing important snow information. (KEYWORDS**:** Snow mapping, Snow Water Equivalent (SWE), bias correction, deep learning, wireless-sensor network

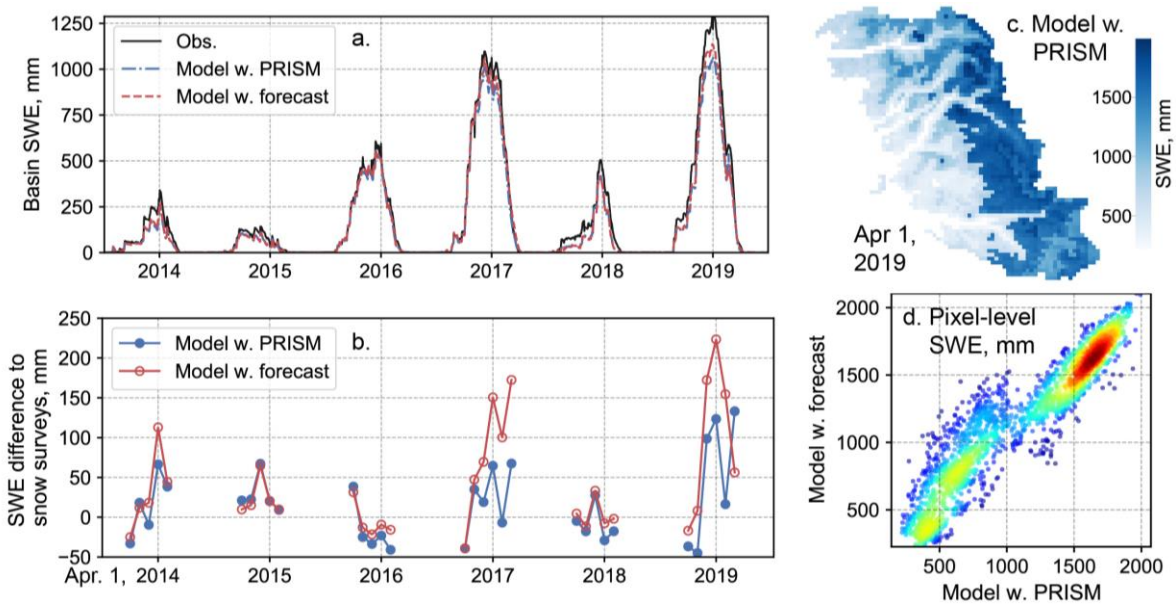

Figure 5. Comparison of SWE estimates by modeling with PRISM data and CNRFC 1-day forecasts. (a) basin-averaged SWE and (b) SWE difference to snow surveys. Taking April 1st 2019 as an example, panel c plots the SWE map by the model with PRISM data, and panel d shows pixel-level SWE comparison.

ACKNOWLEDGEMENTS

This study was supported by the U.S. Bureau of Reclamation WaterSMART Program and the California Department of Water Resources.

REFERENCES

Bales, R. C., Molotch, N. P., Painter, T. H., Dettinger, M. D., Rice, R., & Dozier, J. 2006. Mountain hydrology of the western United States. *Water Resources Research*, *42*(8), 1–13. https://doi.org/10.1029/2005WR004387

Cui, G., Bales, R., Rice, R., Anderson, M., Avanzi, F., Hartsough, P., & Conklin, M. 2020. Detecting rain–snow-transition elevations in mountain basins using wireless sensor networks. *Journal of Hydrometeorology*, *21*(9), 2061–2081. https://doi.org/10.1175/JHM-D-20-0028.1

Henn, B., Musselman, K. N., Lestak, L., Ralph, F. M., & Molotch, N. P. 2020. Extreme runoff generation from atmospheric river driven snowmelt during the 2017 Oroville Dam spillways incident. *Geophysical Research Letters*, *47*(14), 1–14. https://doi.org/10.1029/2020GL088189

Kratzert, F., Klotz, D., Herrnegger, M., Sampson, A. K., Hochreiter, S., & Nearing, G. S. 2019. Toward improved predictions in ungauged basins: Exploiting the power of machine learning. *Water Resources Research*, *55*(12), 11344–11354. https://doi.org/10.1029/2019WR026065

Margulis, S. A., Cortés, G., Girotto, M., & Durand, M. 2016. A Landsat-era Sierra Nevada snow reanalysis (1985–2015). *Journal of Hydrometeorology*, *17*(4), 1203–1221. https://doi.org/10.1175/JHM-D-15-0177.1

Oroza, C. A., Zheng, Z., Glaser, S. D., Tuia, D., & Bales, R. C. 2016. Optimizing embedded sensor network design for catchment-scale snow-depth estimation using LiDAR and machine learning. *Water Resources Research*, *52*(10), 8174–8189. https://doi.org/10.1002/2016WR018896

Zhang, Z., Glaser, S., Bales, R., Conklin, M., Rice, R., & Marks, D. 2017. Insights into mountain precipitation and snowpack from a basin-scale wireless-sensor network. *Water Resources Research*, *53*(8), 6626–6641. https://doi.org/10.1002/2016WR018825

Zheng, Z., Molotch, N. P., Oroza, C. A., Conklin, M. H., & Bales, R. C. 2018. Spatial snow water equivalent estimation for mountainous areas using wireless-sensor networks and remote-sensing products. *Remote Sensing of Environment*, *215*, 44–56. https://doi.org/10.1016/j.rse.2018.05.029